LONG-TERM EFFECTS OF SATELLITE MEGACONSTELLATIONS ON THE DEBRIS
ENVIRONMENT IN LOW EARTH ORBIT

BY

BRIAN PATRICK HARDY

THESIS

Submitted in partial fulfillment of the requirements
for the degree of Master of Science in Aerospace Engineering
in the Graduate College of the
University of Illinois at Urbana-Champaign, 2020

Urbana, Illinois

Adviser:

Adjunct Assistant Professor Koki Ho

ABSTRACT

This thesis examines the potential long-term impacts of satellite megaconstellations in Low Earth Orbit, with a focus on how post-mission disposal rates for megaconstellations will affect their contributions to orbital debris over the next 150 years. A new, medium-fidelity simulation for modeling orbital debris is developed and described, and several test cases are run with SpaceX's Starlink megaconstellation and varying success rates for post-mission disposal. In cases where Starlink's post-mission disposal rate is insufficient to prevent debris growth, varying amounts of active debris removal are explored as a potential mitigation measure. It is shown that LEO debris levels will grow at almost double their baseline rate if Starlink meets only the minimum regulatory requirements for post-mission disposal, and even relatively high rates of active debris removal cannot always return the LEO environment to its non-megaconstellation baseline. Still, the potential exists to minimize the debris-generating effects of large megaconstellations like Starlink if post-mission disposal rates of 95% or better can be achieved.

ACKNOWLEDGMENTS

TABLE OF CONTENTS

LIST OF ACRONYMS

ADEPT	Aerospace Debris Environmental Projection Tool
ADR	Active Debris Removal
ASAT	Anti-Satellite Weapon
DAMAGE	Debris Analysis and Monitoring Architecture to the GEO Environment
DELTA	Debris Environment Long Term Analysis
EOL	End of Life
ESA	European Space Agency
FCC	Federal Communications Commission
GEO	Geostationary Orbit
GPS	Global Positioning System
ISS	International Space Station
JAXA	Japan Aerospace Exploration Agency
LEGEND	LEO-to-GEO Environment Debris
LEO	Low Earth Orbit
LUCA	Long Term Utility for Collision Analysis
MASTER	Meteoroid and Space Debris Terrestrial Environment Reference
MEDEE	Modeling the Evolution of Debris on Earth's Environment
NASA	National Aeronautics and Space Administration
NEODEEM	Near-Earth Orbital Debris Environmental Evolutionary Model
ODMSP	Orbital Debris Mitigation Standard Practices
ODPO	Orbital Debris Program Office
PMD	Post-Mission Disposal
SATCAT	Satellite Catalog
SDIRAT	Space Debris Impact Risk Analysis Tool
SGP4	Simplified General Perturbations Version 4
SSN	Space Surveillance Network
UCS	Union of Concerned Scientists
UMPY	Undisposed Mass Per Year

CHAPTER 1: INTRODUCTION

1.1   Motivation

Much of the advanced technology and global interconnectivity enjoyed in the modern era is dependent on distant, often unseen assets: artificial satellites. The public is perhaps most cognizant of the role of telecommunication satellites, providing television and radio services, as well as navigation satellites like the Global Positioning System (GPS). Still, beyond these well-known roles, the more than 2000 active spacecraft today support a myriad of other services including imaging, weather forecasting, and astronomy [1]. An inspiring example is the International Cospas-Sarsat Program, a multinational satellite network that detects radio distress beacons and has helped rescue more than 40,000 people since the 1980s [2]. Recently, however, a new paradigm for satellite systems has begun to emerge. Multiple companies have announced constellations with hundreds or thousands of satellites, so-called "megaconstellations," which may triple the number of active spacecraft in coming years. Unfortunately, as satellite networks increase in scale, they face a growing and potentially catastrophic threat: orbital debris.

Though near-Earth space appears vast and relatively empty, the threat posed by orbital debris is very real. The NASA Orbital Debris Program Office (ODPO) is aware of more than 23,000 pieces of debris larger than 10 cm, and it is estimated that there are more than 100,000,000 pieces of debris larger than 1 mm [3]. Though the risk of collision is small for a given object over short time periods, this probability is amplified when considering the entire satellite population over long timeframes. A particular vulnerable segment of near-Earth space is Low Earth Orbit (LEO), where almost three quarters of active satellites operate [1]. On-orbit collisions can and do happen in LEO, with results ranging from disabled instruments to catastrophic breakups that

introduce even more debris. The latter result, implying that past collisions increase the risk of future collisions, is of particular concern for spacecraft operators in LEO.

Since collision risk is directly related to the number of orbiting objects, the advent of megaconstellations has attracted scrutiny from government regulators and the satellite community at large. Companies including Amazon, OneWeb, and SpaceX have all begun development of megaconstellations with hundreds or thousands of satellites in LEO, designed to provide high-speed Internet connectivity around the globe [4] [5] [6]. SpaceX and its 4425-satellite Starlink constellation present a particularly interesting case study, as Starlink is thus far the largest megaconstellation to receive approval from the Federal Communications Commission (FCC). Starlink also has a significant lead over its competitors, with over 400 satellites launched as of April 2020 [7]. Nonetheless, there remain interesting questions regarding the potential impacts of Starlink or other megaconstellations on the LEO debris environment.

With concepts still in their early stages, the flight-proven reliability of megaconstellation satellites remains under study. Even a small failure rate, when applied across thousands of objects, has the potential to leave behind large numbers of uncontrolled satellites that contribute to the LEO debris environment. This thesis aims to develop a model to study the long-term effects of megaconstellations on the LEO debris environment, with a particular focus on the Starlink network. A key focus is how Starlink's post-mission disposal (PMD) rate affects debris growth over time, as well as how different debris mitigation strategies affect Starlink operations in the short term (20 years) vs. the entire LEO environment in the long term (150 years). Finally, varying levels of active debris removal (ADR) are investigated as a potential solution for debris growth induced by megaconstellations. The remainder of this introduction provides additional background information on orbital debris, megaconstellations, and active debris removal.

1.2   The Orbital Debris Environment

Today's active satellites are significantly outnumbered by the debris accumulated in Earth orbit over the past half-century. This orbital debris varies in composition, from discarded lens caps to entire spacecraft, but is generally defined by NASA as "any human-made object in orbit about the Earth that no longer serves any useful purpose" [3]. In the United States, responsibility for detecting and tracking debris falls to the Space Surveillance Network (SSN). The SSN maintains a public catalog of unclassified, Earth-orbiting objects via its worldwide network of telescopes and radar stations. Unfortunately, SSN observations are limited to objects larger than 10 cm, and the extent of smaller debris can only be estimated by observing returned spacecraft or conducting time-consuming measurements with more sensitive instruments [8]. Figure 1 displays the history of objects in the public SSN catalog, from the 1957 launch of Sputnik to present day.
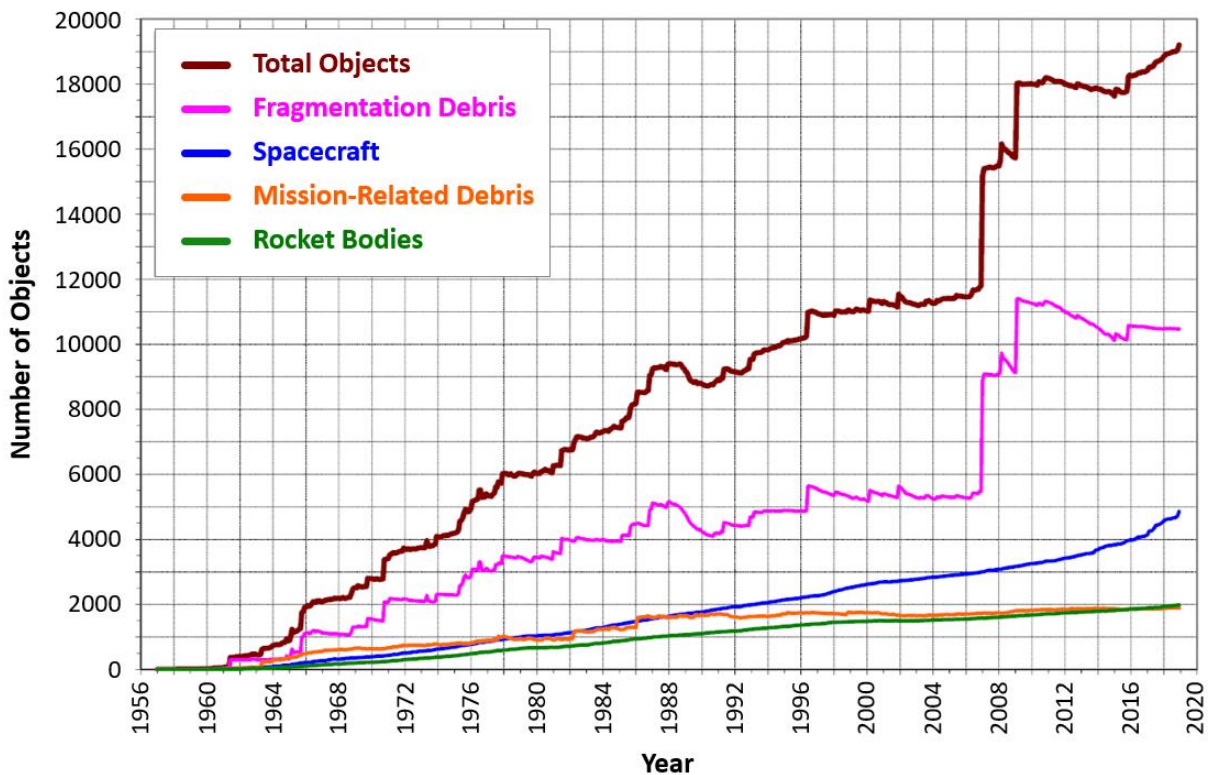

Figure 1: History of Cataloged Objects in Earth Orbit [9]

As shown in Figure 1, the amount of debris in Earth orbit has increased with little interruption over the past 60 years. In addition, roughly two-thirds of the objects in Figure 1 are orbiting in LEO [10]. Large pieces of debris include defunct satellites and rocket upper stages, with both sometimes exploding due to aging batteries and pressure tanks. Smaller debris arises from many sources, including discarded satellite mechanisms, erosion from spacecraft surfaces, and explosions as mentioned above. Finally, debris of all sizes can be generated in large quantities from collisions and intentional breakups. Though many sources exist for orbital debris, there remains only one natural removal mechanism: atmospheric drag. Debris lifetimes vary from months to decades at orbits below 600 km, but above this point atmosphere drag is too weak to offset the production of new debris [8]. At these higher orbits, debris may persist for centuries.

Though rare, collisions and intentional breakups have become major contributors to orbital debris, and several incidents are worth highlighting. Intentional breakups are typically associated with tests of anti-satellite weapons (ASAT). These systems have been demonstrated by multiple militaries, including the United States, but a January 2007 ASAT test by China in particular sparked international outcry for its contribution to debris. The destruction of the Fenyun 1C satellite by a ballistic missile generated over 3400 new cataloged objects, amounting to one-sixth of all radar-trackable debris [11]. The breakup of Fengyun 1C was followed by another unrelated debris incident in February 2009, when the first satellite-to-satellite collision in history occurred between the still-operating U.S. satellite Iridium 33 and defunct Russian satellite Cosmos 2251. The hypervelocity impact destroyed both spacecraft and produced a debris field of 2200 new cataloged objects [12]. Alarmingly, Iridium 33 was still maneuverable at the time, but prediction software did not rank the expected close approach as significant [13]. The Iridium-Cosmos collision further highlights the dangers posed by orbital debris to operating spacecraft.

Though major collisions and breakups are infrequent, the fragments they generate only add to the debris population that must continually be avoided by operating spacecraft. Collision avoidance is a vital element of modern satellite operations. For example, the European Space Agency (ESA) reports that each week it receives approximately two close encounter alerts from the SSN for each satellite in its LEO fleet. Each alert then requires a detailed analysis to assess collision risk, and avoidance maneuvers are executed for any risks greater than 1 in 10,000 [14]. In one extreme case in 2012, a piece of debris from the Iridium-Cosmos collision passed close enough to the International Space Station (ISS) to force the crew to shelter in their return capsule as a precaution [15]. When weighing the need for a collision avoidance maneuver, the stakes are high. Consider that just a 1-gram fleck of paint, traveling at orbital speeds of 10 km/s (2200 mph), can easily exceed the kinetic energy of a bullet. Finally, even when collision avoidance maneuvers are successfully executed, they still consume valuable propellant and operating time.

Recognizing the need to reduce hazards for future spacecraft, several governments have enacted debris mitigation policies in recent decades. The U.S. Orbital Debris Mitigation Standard Practices (ODMSP), for example, require operators to minimize mission-related debris, passivate spacecraft to reduce explosions, and maneuver aging spacecraft to less-occupied orbits (so-called "graveyard orbits") or altitudes where re-entry will occur within 25 years [16]. Still, the ODMSP and similar policies have only been in effect since the early 2000s, and their reach is limited. ESA estimates that 40% of LEO spacecraft do not meet international guidelines for debris mitigation [17]. Tightening existing restrictions has also proven controversial, with the FCC deferring an April 2020 decision on stricter orbital debris criteria due to industry opposition [18]. In any case, as long as collision avoidance and spacecraft disposal systems remain imperfect, satellites in LEO will continue to face risks from orbital debris.

1.3   History of Megaconstellations

As online services become increasingly central to modern life, there remains a growing digital divide between those with and without internet access. Recent studies show that while 87% of the developed world is online, this figure drops to 47% for the developing world and 19% for the least developed countries [19]. Even in the United States, which has widespread internet access, the FCC estimates that 19 million Americans in remote areas still lack high-speed, broadband connections [20]. Satellite internet aims to close the gap by reaching these remote areas, where ground-based infrastructure is either nonexistent or insufficient to provide broadband speeds.

To date, satellite internet has predominantly been delivered by large spacecraft in geostationary orbits (GEO). Orbital altitude is a trade-off though; while higher orbits like GEO allow operators to provide coverage with a handful of satellites, the long transmit distances create connection lag. Satellite megaconstellations propose a new approach that uses small satellites at lower altitudes to achieve almost fiber-optic internet speeds. The catch is that hundreds to thousands of satellites are needed to achieve global, redundant coverage in LEO [21]. Nevertheless, with the satellite internet market projected to reach $400 billion by 2040 [22], several companies have announced plans for megaconstellations. Table 1 details three of the largest megaconstellations under development by Amazon, OneWeb, and SpaceX.

Table 1: Planned Satellite Megaconstellations, as of April 2020

Operator	Constellation	Number of Satellites			Sources
		Launched	Approved*	Applied For*	
Amazon	Kuiper	0	0	3236	[4]
OneWeb	OneWeb	74	720	1260	[5] [23]
SpaceX	Starlink	422	4425	42,000	[6] [7]

* Refers to frequency licensing with the FCC, required for all U.S. satellites

Though constellations with dozens of commercial satellites are nothing new in LEO, as shown in Table 2, megaconstellations are rapidly shifting the rankings. In just one year since their first launches, OneWeb and SpaceX have already matched or outpaced many well-known operators. Remarkably, these recent launches represent only about 10% of the final size of each megaconstellation, and the completion of SpaceX's Starlink network alone would triple the number of satellites currently in orbit. With OneWeb's future uncertain following bankruptcy [23] and Amazon's Kuiper network still awaiting FCC approval, Starlink will serve as the primary megaconstellation studied in this thesis.

Table 2: Largest Constellations of Commercial Satellites, as of April 2020

Operator	Constellation	No. Active Satellites	Orbit	First Launch	Purpose & Sources
SpaceX	Starlink	422	550 km	May 2019	Broadband Internet [7] [24]
Planet	Dove, SkySat, RapidEye	150	400-700 km	Apr. 2013	Remote imaging [25] [26]
Spire Global	LEMUR	84	400-600 km	Sep. 2015	Weather data, aircraft & ship tracking [27] [28]
Iridium	Iridium NEXT	75	780 km	Jan. 2017	Voice & data services [29] [30]
OneWeb	OneWeb	74	1200 km	Feb. 2019	Broadband Internet [23] [24]

As the largest megaconstellation to receive FCC approval thus far, Starlink is an opportune test case for studying how megaconstellations may affect the LEO debris environment. Starlink's orbital parameters have varied significantly as SpaceX continues to refine the design, but this thesis will focus on the most recent FCC approval in December 2019 for 1584 satellites at 550 km and 2825 satellites at 1110-1325 km [6]. It should be noted that SpaceX is currently petitioning the

FCC to operate all its satellites at the lower 550-km orbit, but this application has yet to be approved and may face opposition from other operators [31]. As will be shown later, Starlink's choice of altitude may be critical in determining its long-term contributions to LEO debris.

There are several mechanisms by which megaconstellations like Starlink can affect the debris environment. First, active Starlink satellites will continually be subjected to LEO debris and could themselves be disabled or destroyed. This scenario is considered less likely, as SpaceX has taken admirable steps to implement collision avoidance in all stages of flight [6]. The risk remains, however, as highlighted by a March 2019 encounter between an ESA satellite and Starlink that necessitated an avoidance maneuver [32]. Still, the greater concern is not regarding active Starlink satellites, but rather satellites that fail to deorbit properly at the end of their lives. The ODMSP debris mitigation guidelines, also followed by NASA and the FCC, require a 90% success rate for post-mission disposal into the atmosphere or a graveyard orbit [16]. If only the minimum PMD requirement is met for a megaconstellation as large as Starlink, hundreds of failed satellites could become orbital debris. Though SpaceX is aiming for the highest PMD rates possible, it is still too early in Starlink's deployment to assess the actual failure rate over time.

1.4 Active Debris Removal

As megaconstellations insert potentially thousands of satellites into an ever-growing debris environment, there is a renewed need to actively counter debris growth to preserve the future LEO environment. Recent studies have shown that even with aggressive implementation of post-mission disposal and explosion mitigation, the debris environment in LEO will continue to grow over the next two centuries [33]. One proposed solution is active debris removal, whereby special-purpose spacecraft capture existing debris to reduce future collision rates. With careful selection criteria for what debris is targeted and removed, there are both present and future benefits of ADR.

Removing debris in the 5-mm-to-1-cm range can reduce ongoing threats to most operational spacecraft, while removing larger objects like defunct satellites and upper stages can eliminate the largest "debris generators" and lower future population growth [34]. The ADR strategies explored in this thesis will assume the latter removal strategy.

Simple in theory, ADR remains a challenging endeavor and has never been successfully demonstrated. Various ideas for ADR have been floated, with proposals ranging from attaching drag-enhancement devices to actively bringing the target debris all the way into the atmosphere. Whatever method is implemented, one of the primary technological hurdles is grappling non-cooperative, tumbling debris objects [34]. Finally, even once ADR technology is successfully demonstrated, there are legal and political hurdles as well. The Outer Space Treaty implies that spacecraft remain the property of the launching state even after operations cease, which significantly complicates the question of whether nations can unilaterally remove debris that is not their own [35]. (As an aside, the reverse question is also interesting: whether a nation can be held liable for damage caused by its own debris.) Still, in spite of technical and legal difficulties, active debris removal could prove vital to preserving the future LEO environment.

1.5 Thesis Structure

The previous sections introduced the motivation for this thesis and provided background information on orbital debris, megaconstellations, and active debris removal. In the next chapter, a literature review summarizes the study of the orbital debris environment over the past several decades. The third chapter then details a new simulation developed to model the long-term debris environment in LEO, with options for varying levels of megaconstellation PMD and ADR. Finally, the fourth chapter presents simulation results for several test cases with the Starlink megaconstellation, and the fifth chapter closes with conclusions and suggestions for future work.

CHAPTER 2: LITERATURE REVIEW

2.1 Overview

In the past forty years, an extensive body of literature has developed surrounding the study of orbital debris, megaconstellations, and active debris removal. Notable publications are summarized in the sections below, beginning with foundational work in the 1970s and 1990s. Later work on orbital debris and megaconstellations is then divided into two categories: semi-analytical, statistical modeling vs. high-fidelity simulations. In the former category, the literature typically models the LEO environment via source-sink differential equations or statistical estimations of collision rates. The latter category, on the other hand, is defined by computational-intensive simulations with full force orbit propagation. Finally, the literature review concludes by summarizing recent publications on the effects of active debris removal, including an interesting series of studies that approach the problem from a game theoretical perspective.

2.2 Early Studies of Orbital Debris

The study of the orbital debris environment first came to prominence in 1978 with the work of Kessler and Cour-Palais. This study built on prior experience with modeling the asteroid belt and its growth due to mutual collisions, a phenomenon that the authors recognized could also occur among Earth-orbiting debris. By examining historical data and previous work on hypervelocity impacts, Kessler and Cour-Palais created one of the first breakup models for on-orbit collisions and derived relationships between satellite mass and cross-sectional area. These relationships were then implemented in a satellite environment model, which used spatial density distributions to estimate collision rates in Earth orbit and the growth of orbital debris over time. Based on results from this model, Kessler and Cour-Palais correctly predicted that collision fragments would

become a significant source of debris by the year 2000. More importantly, their work was the first to suggest that certain Earth orbits could potentially reach a "tipping point" where the growth of debris becomes exponential over time [36]. The latter conclusion was groundbreaking at the time, and the scientific community adopted the term "Kessler syndrome" to describe the potential for exponential debris growth in Earth orbit.

Another cluster of studies on orbital debris followed in the 1990s, in response to plans for large telecommunications constellations like Iridium and Globalstar. In 1997, Rossi et al. studied the debris-generating effects of these constellations using a semi-deterministic model with a statistical, "particle-in-a-box" approach for estimating collision probabilities. This work concluded that LEO collision rates would not increase significantly if new constellations employed post-mission disposal, but that rates could rise by 45% without PMD [37]. Subsequent work in 1999 by Rossi et al. focused on the impacts of a hypothetical collision in the 66-satellite Iridium constellation, ironically only ten years before such an event would actually occur. It was noted that large constellations are at particular risk for cascading collisions, due to their use of multiple orbital planes with varying precession rates [38]. Regarding debris growth, Mendell et al. also concluded that satellite-debris collisions appeared to be more impactful than satellite-satellite collisions [39]. Though many of the studied constellations like Iridium ultimately fell into bankruptcy, they set a precedent for the megaconstellations that followed twenty years later.

These early studies offered the first evidence of an ever-growing debris population, but there are limitations to the pre-2000 literature. The number of cataloged objects in orbit has more than quadrupled since the first work of Kessler and Cour-Palais, and large constellations studied in the 1990s are still an order of magnitude smaller than modern megaconstellations. To accurately evaluate the impact of megaconstellations in LEO, an up-to-date object catalog is critical.

11

2.3   Semi-Analytical & Statistical Modeling

Though less detailed than high-fidelity simulations, semi-analytical and statistical models generally run much faster and can provide valuable, first-order results when studying the orbital debris environment. Over the past decade, a variety of publications have applied these methods specifically to studying the debris-generating effects of megaconstellations. Pardini and Anselmo's model, developed in 2014, estimated satellite collision rates with a particle-in-a-box approach similar to that used previously by Rossi et al, Kessler, and Cour-Palais. This statistical approach relies on modeling cataloged objects as "particles" interacting inside discretized "boxes" (i.e. orbital shells in LEO), with collision activity directly related to the density of objects [12]. Recently, Anselmo and Pardini applied their model to study how modern-day collision rates would be affected by replacing existing, large satellites with hundreds of small satellites. Particular emphasis was placed on how many new, uncontrolled satellites (i.e. undisposed satellites) could be added to LEO before collision rates grew by 10%. While about 500 uncontrolled satellites were needed to cause this increase in 1200-km orbits, only 100-200 satellites were necessary in popular orbits near 800 km [40]. A separate publication by Pardini and Anselmo, instead using the Space Debris Impact Risk Analysis Tool (SDIRAT) to estimate collision rates, revealed similar results. The authors concluded that megaconstellations will require a minimum PMD rate of 90% and ideally approaching 99% [24]. This finding is mirrored in many studies; namely, that the impact of megaconstellations on debris generation is strongly correlated to disposal success.

While Pardini and Anselmo focused primarily on modeling the effects of large numbers of generic satellites, there are a variety of recent publications regarding specific megaconstellations as well. A notable area of study has been estimating collision rates within the OneWeb and Starlink megaconstellations. Radtke et al. and Le May et al. applied Poisson statistics to debris fluxes from

ESA's Meteoroid and Space Debris Terrestrial Environment Reference (MASTER) model, allowing them to compute collision probabilities over varying timeframes. Radtke et al. found that the chance of a catastrophic collision involving OneWeb was 35% across the system's lifetime [41], while Le May et al. predicted a 46% chance of a catastrophic collision between Starlink and a non-cataloged object over a 5-year period [42]. The latter result is particularly interesting, as it suggests that megaconstellations will face a significant threat from orbital debris that cannot be tracked by current space surveillance networks. Foreman et al. predicted that the initial 1600 spacecraft in Starlink will experience 68 encounters with debris larger than 1 cm, many of which could be below the SSN's 10-cm detection threshold [35]. These studies further demonstrate that the threat of orbital debris is mutual, affecting both the overall LEO environment as well as megaconstellations themselves.

Predicting collision rates in LEO is a valuable tool in studying the impact of megaconstellations, allowing one to understand near-term increases in collision risk and giving satellite operators a reference for how many avoidance maneuvers they might expect. Nevertheless, existing semi-analytical and statistical models typically only capture the short-term impacts on the LEO debris environment, and debris growth into the far future is not considered. To understand the future impact of increased collision rates, as well as study potential mitigation strategies like active debris removal, one must turn to numerical simulations.

2.4   High-Fidelity Simulations

Numerical simulations allow researchers to propagate thousands of individual LEO objects and study their interactions over multi-century timescales. These simulation tools are critical for studying the long-term evolution of the LEO debris environment, and several such tools are actively in use by space agencies around the world. One of the most well-known contributors to

the field is the NASA Orbital Debris Program Office, which recently completed a study of megaconstellations in 2018. This work by Liou et al. used the ODPO's LEO-to-GEO Environment Debris (LEGEND) model to study the potential debris contributions from a 20-year megaconstellation with 8300 satellites and a 50-year megaconstellation with 6700 satellites. Results from the 20-year case are shown in Figure 2 below, where even a 95% PMD rate for the megaconstellation still resulted in twice as much orbital debris as the baseline case after 200 years. The ODPO concluded that a 99% PMD rate for megaconstellations will be required to mitigate future debris generation, though they noted diminishing returns for 99.9% PMD [43]. As this study contains some of the most recent and high-fidelity simulations involving megaconstellations, it also serves as a reference point for validating the new simulation developed in this thesis.
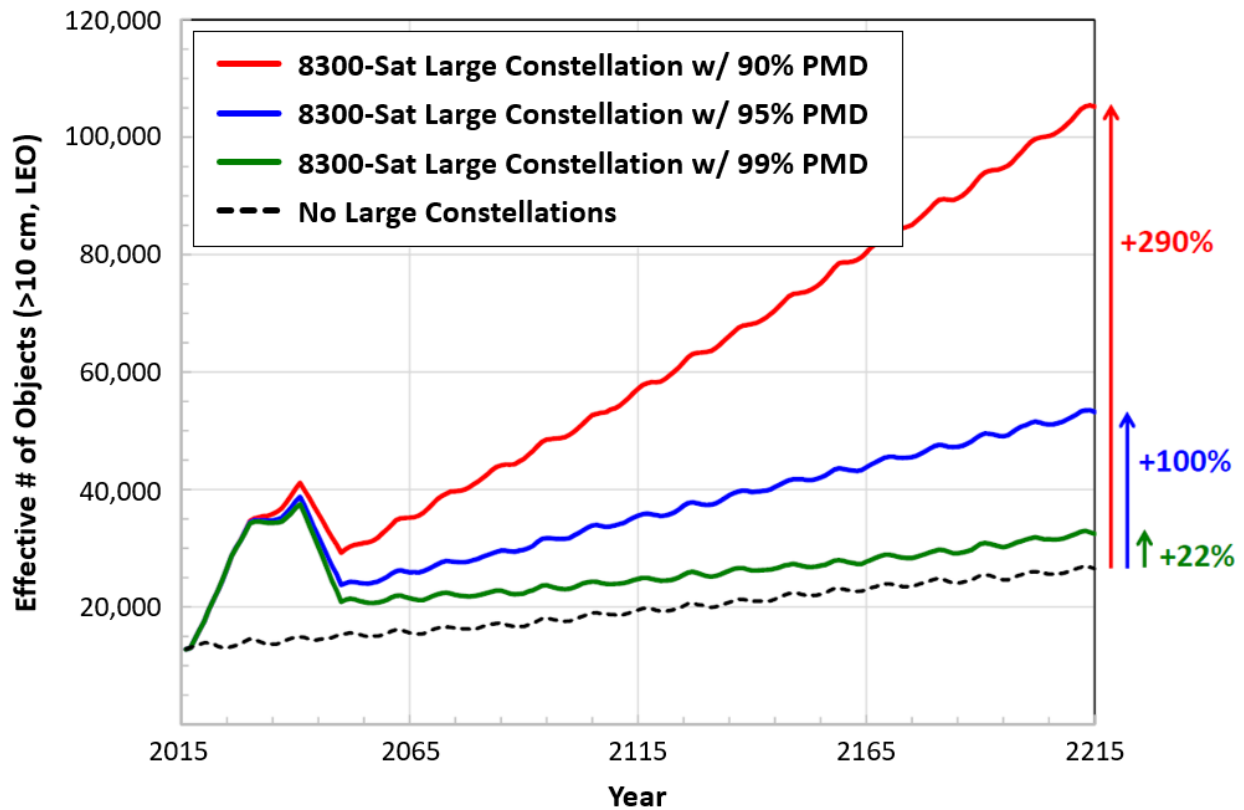

Figure 2: ODPO Study of Varying PMD Rates for a 20-Year Megaconstellation [42]

14

An earlier but similar study, with a smaller megaconstellation, was undertaken by Bastida Virgili et al. in 2016. This work included 200-year simulations of the LEO debris environment assuming the addition of a generic, 1080-satellite megaconstellation that operates from 2021-2071. Results were averaged from four different simulation tools: Modeling the Evolution of Debris on Earth's Environment (MEDEE), Long Term Utility for Collision Analysis (LUCA), Debris Analysis and Monitoring Architecture to the Geosynchronous Environment (DAMAGE), and Debris Environment Long Term Analysis (DELTA). As shown in Figure 3, a key area of study was again how a megaconstellation's PMD rate would affect its long-term impact on the LEO debris environment [44]. Though the results from Bastida Virgili et al. are less dramatic than the ODPO study, owing to the smaller size of the megaconstellation, they still demonstrate significant debris growth for any PMD rates below 90%.
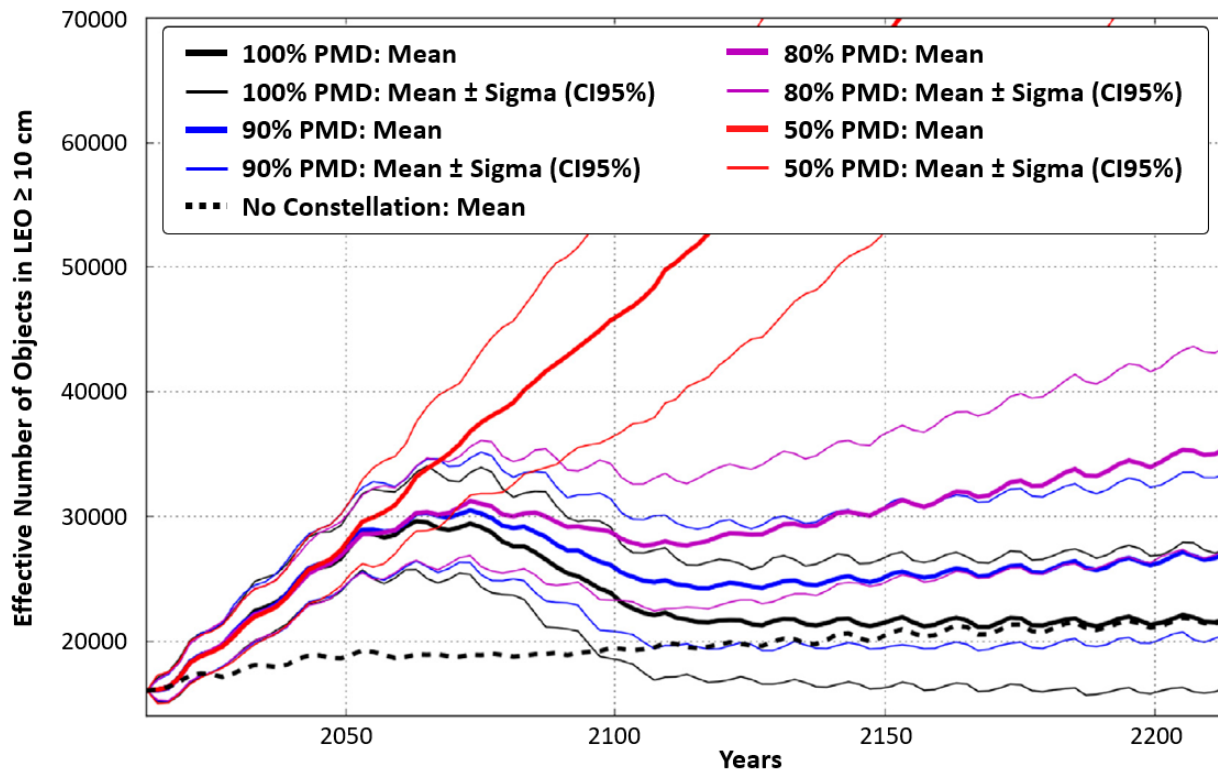

Figure 3: Study of Varying PMD Rates for a 50-Year, 1080-Satellite Megaconstellation [44]

Whether the result of short satellite lifetimes or failed post-mission disposal, the undisposed mass left behind by megaconstellations is cited by several publications as a key driver of debris growth. Henning et al. found undisposed mass per year (UMPY) to be a strong evaluation metric for megaconstellations and simulated a range of UMPY rates using the Aerospace Debris Environment Projection Tool (ADEPT). The number of LEO objects after 200 years was shown to grow linearly as a function of UMPY rates less than 10,000 kg/year, with the relationship becoming quadratic thereafter [45]. Finally, even when PMD systems work successfully, the choice of disposal strategy can also have an impact on long-term debris growth. Using the previously-mentioned DAMAGE tool, Lewis et al. found that using powered reentry (i.e. near-immediate disposal) instead of 25-year disposal orbits for OneWeb satellites would reduce catastrophic collisions by 52% [46]. These publications agree that large numbers of uncontrolled satellites with long lifetimes, such as those left behind by megaconstellations with sub-optimal PMD rates, may pose a significant hazard to the future LEO environment.

High-fidelity simulations represent the most detailed models of orbital debris developed to date, and they can offer valuable insight on the future of the space environment. Nevertheless, a lack of public availability and large computational requirements remain the greatest limitations of many modern simulation tools. Significant computational power is required to propagate orbits and perform conjunction analyses for thousands of space objects, particularly over multi-century timescales, and developing a simulation of this complexity was considered infeasible in the time available. Instead, as will be shown later, the numerical simulation developed for this thesis focuses on achieving a medium level of fidelity by combining elements of both numerical simulations and the statistical methods discussed previously.

2.5   Effects of Active Debris Removal

Lastly, a significant body of literature has also explored the potential benefits of active debris removal in the LEO environment. A NASA ODPO study in 2010 demonstrated a 75% increase in the LEO population by 2210 without active debris removal, whereas removing five high-risk objects per year could maintain debris at existing levels. This study leveraged previous work which showed that the product of mass and collision probability was a good criteria for selecting what debris to remove [33]. Still, active debris removal is only effective to a point, with Lewis et al. demonstrating diminishing returns as ADR rates increased [46]. There also remains significant debate regarding the best method for removing debris, with some favoring drag-enhancement devices to reduce orbital lifetimes. Using JAXA's Near-Earth Orbital Debris Environmental Evolutionary Model (NEODEEM), Kawamoto et al. showed that the large sizes of drag-enhancement devices may increase collisions in the short term but ultimately lead to reductions in overall debris [47]. Regardless of what method is used, recent literature agrees that active debris removal could prove critical to safeguarding the future LEO environment.

Another interesting perspective on active debris removal involves the application of game theory by Klima et al. in a series of publications in 2016 and 2018. The authors created their own high-fidelity orbital debris model using the Simplified General Perturbations Version 4 (SGP4) propagator, the well-known "Cube approach" for conjunction analysis, and the NASA Standard Breakup Model for collision modeling. From there, empirical game theory was used to study the optimal strategy for several state actors performing varying levels of active debris removal [48]. A key finding was that often the best debris removal strategies involved actors with a disproportionately large number of orbiting assets, suggesting that a coordinated global approach

to debris removal would be more effective that individuals acting alone [49]. This work suggests that international cooperation will be a key element of any future ADR programs.

Although active debris removal has been studied in a variety of literature, there are relatively few studies on its potential use as a mitigation measure for debris generated by megaconstellations. A notable exception is Lewis et al. and their analysis of actively removing failed OneWeb satellites, but the OneWeb system is still significantly smaller than other planned megaconstellations like Amazon's Kuiper and SpaceX's Starlink. In addition, the ADR portion of the study only considered a baseline PMD rate of 95% [46]. Going forward, one of the primary goals in this thesis is to study a range of PMD and ADR rates for megaconstellations, with a particular focus on what ADR rate is required to restore the baseline debris environment when megaconstellation PMD rates are sub-optimal. This analysis is carried out via a new, medium-fidelity tool for simulating the LEO debris environment, as discussed in the next chapter.

CHAPTER 3: METHODOLOGY

3.1   Simulation Framework

To study how megaconstellations may affect the long-term debris environment in LEO, a Python-based simulation was created to combine the benefits of existing high-accuracy simulations and statistical modeling. A flow chart of this new, medium-fidelity simulation is provided in Figure 4. The basic framework begins by initializing the LEO background population and defining launch schedules for both standard satellites and megaconstellations. Then, at discrete time steps, the orbits of individual objects are decayed (i.e. lowered due to atmospheric drag), and some active objects are removed due to successful post-mission disposal. On-orbit collisions are triggered by comparing a random number generator against statistically-derived collision probabilities. New collisions, new launches, and active debris removal continually add and subtract objects from the overall population, and the simulation steps repeat until an end time is reached. In summary, by considering only orbital decay and statistical collision probabilities, this new simulation is able to model long-term debris evolution while avoiding time-consuming orbit propagation and conjunction analysis across thousands of objects.

A variety of settings can be modified within the simulation, but the most important for this thesis are the megaconstellation PMD and ADR rates. All simulations assume a 150-year runtime from 2020 to 2170, with SpaceX's Starlink megaconstellation operating during the first 20 years. The time step for orbit propagation and collision analysis is set at five days. As there is a certain degree of randomness in determining the magnitude and timing of on-orbit collisions, a Monte Carlo analysis averages the results of 100 simulation runs for any given test case. The remaining sections of this chapter provide further details on each aspect of the simulation.
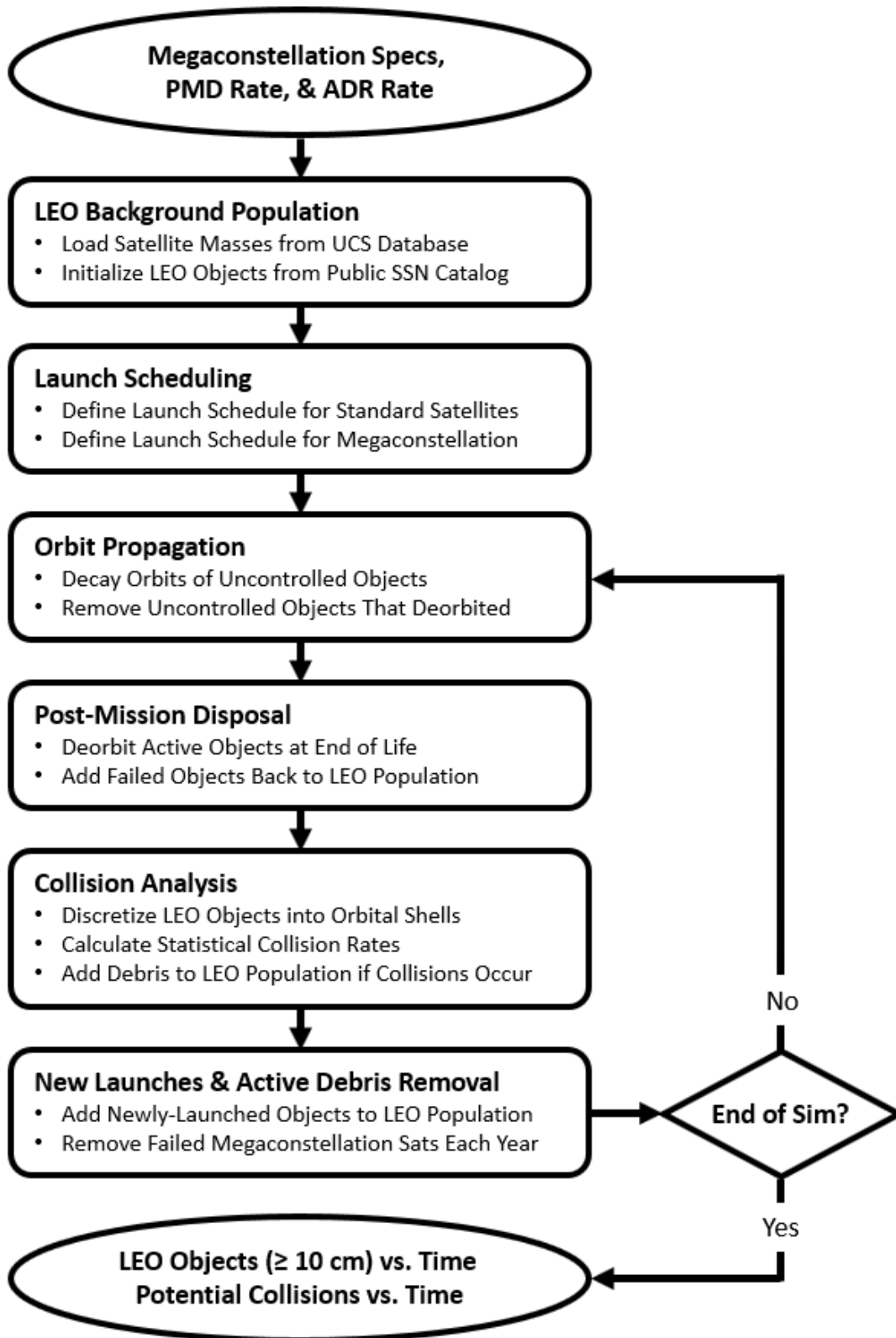
19

Figure 4: Flow Chart for Orbital Debris Simulation

3.2 LEO Background Population

The first step in the simulation is to define all existing objects in LEO at the start time. Information on orbiting objects is sourced from CelesTrak's distribution of the public SSN catalog, also known as the Satellite Catalog (SATCAT) [10]. The SATCAT provides a variety of information for each cataloged object including operational status, launch date, decay date (if applicable), apogee, perigee, and radar cross section. After parsing the database to ignore objects that are already decayed or not yet launched as of January 2020, all remaining objects are split into three groups: active, non-operational, and debris. The former two groups include intact objects like satellites and upper stages, with active objects identified by their SSN status code. An additional parser ignores any objects not in LEO, i.e. with semi-major axis greater than 2000 km. The resulting initial LEO population of 14,687 objects is shown in Figure 5.
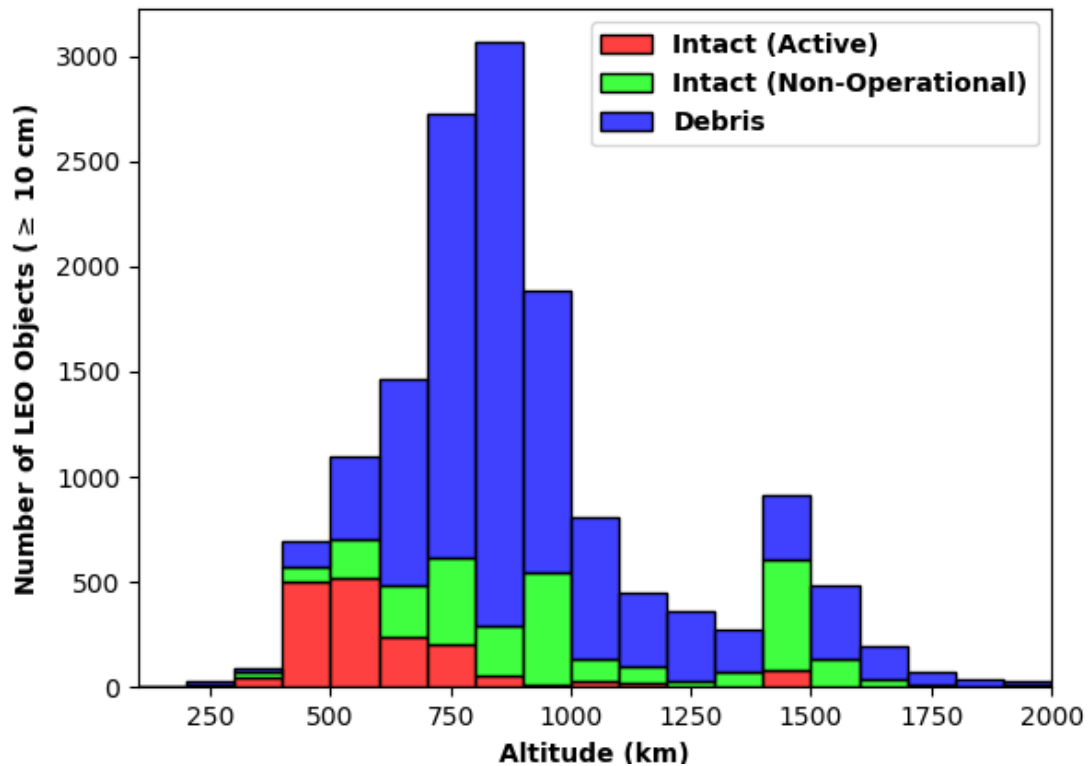

Figure 5: LEO Background Population on January 1, 2020 [10]

When initializing the LEO background population, every object is assigned an orbital altitude, cross-sectional area, and mass. Orbital altitude is defined as the average of the apogee and perigee values obtained from the SATCAT. As the majority of LEO objects are in low-eccentricity orbits [49], the simulation assumes circular orbits defined entirely by these altitude values. Additional orbital parameters are ignored, as it is assumed that collision rates are driven primarily by object densities as a function of altitude. Unfortunately, while an object's altitude is relatively easy to pinpoint, determining cross-sectional area and mass is more difficult. An object's cross-sectional area can differ by orders of magnitude compared to its SSN-provided radar cross section [36], and the SATCAT does not provide mass data for cataloged objects. Instead, both of these parameters must be estimated by other means.

When determining cross-sectional area and mass, intact and debris objects take opposite approaches. For intact objects, both active and non-operational, it is assumed that mass is known with some accuracy from existing databases and literature. The mass of active objects is found by searching the Union of Concerned Scientists (UCS) Satellite Database, which contains details on all operational satellites as of December 2019. If an active object's mass is not listed in the UCS database, it is assumed to be the database average: approximately 1500 kg [1]. The mass of all non-operational objects is assumed to be 700 kg, based on recent estimates for the average mass of intact objects [40] and the current numbers of active vs. non-operational objects in LEO. Once mass is known, cross-sectional area for intact objects is calculated by inverting the classical relationship shown in Equation 1 [50].

$$M = 62.013A^{1.13} \qquad (1)$$

where M is mass [kg] and A is cross-sectional area [m^2]. Again, the driving mentality for intact objects is to estimate mass and then calculate the corresponding cross-sectional area.

In contrast with intact objects, debris objects assume that cross-sectional area can be estimated relatively well from existing data, and then a corresponding mass can be calculated. This method was chosen primarily because there is a significant amount of literature concerning the estimation of debris cross-sectional area based on radar cross sections. Thus, if a radar cross section is provided for a debris object in the SATCAT, then its cross-sectional area is calculated via Equation 2 from literature [51].

$$A = 0.571(RCS)^{0.767} \tag{2}$$

where A is cross-sectional area and RCS is radar cross section. If a radar cross section is not provided, the cross-sectional area is assumed to be that of a 10-cm sphere – the detection threshold of the SSN. Once cross-sectional area is determined, the mass of the debris object is then calculated via Equation 1.

Finally, for active objects only, a fourth parameter is stored: the end-of-life (EOL) timestamp. This value informs the simulation when an active object should initiate post-mission disposal, assumed to be 10 years after launch for a standard, non-megaconstellation satellite. Importantly, it is assumed that all active objects at least attempt post-mission disposal at the end of their lifetimes. Though not true for many satellites today [17], this assumption effectively creates a best-case scenario for future debris generation. In doing so, the effects of megaconstellations are more prominent and easily-studied.

3.3 Launch Scheduling

Once the background LEO population is initialized, the simulation then defines future launch schedules for standard satellites and megaconstellations. Standard satellites are assumed to continually repeat the historic 10-year launch record from 2010-2020, with launches including both active objects (i.e. operating satellites) and non-operational objects (i.e. upper stages). This

launch record is generated from the SATCAT using the same methods described previously for determining altitude, cross-sectional area, and mass. In addition, a future launch date is also saved for each object.

As discussed previously, SpaceX's Starlink network was chosen as the representative example for megaconstellations in this thesis. The number of Starlink satellites at varying altitudes was sourced from its most recent FCC approval [6], while cross-sectional area and mass were sourced from prior FCC applications [52] and recent SpaceX press releases [53]. A summary of technical specifications is provided in Table 3.

Table 3: Technical Specifications for Starlink Megaconstellation [6] [52] [53]

Orbital Altitude (km)	550	1110	1130	1275	1325
Number of Satellites	1584	1600	400	375	450
Cross-Sectional Area (m^2)	15.45				
Mass (kg)	260				

In determining a long-term launch schedule for Starlink, it was assumed that SpaceX will continue its current trend of launching 60 satellites per month [53]. From there, it was further assumed that the network will be built outward from 550 km to 1325 km and that no launch can carry satellites in multiple orbital shells. Applying these assumptions, one arrives at a schedule of 76 monthly launches in order to complete Starlink. This launch schedule is then repeated such that each satellite is replaced after 6 years and 4 months, well within the useful lifetime of 5-7 years cited by SpaceX [52]. Determining a lifetime for the overall Starlink network was difficult, given a lack of public information, but for this analysis it is assumed that launches cease after 20 years. Though it is very possible that some form of Starlink may operate beyond this point, the system would likely be upgraded in some way that would invalidate further analysis.

3.4 Orbit Propagation

The iterative component of the simulation, i.e. the code that executes at every time step, begins with updating the orbital altitudes of all non-operational and debris objects. These objects are uncontrolled and will naturally lose altitude over time due to atmospheric drag, an effect known as orbital decay. Once an uncontrolled object's altitude decays below 100 km, it is assumed to have deorbited and is removed from the simulation. Active objects, on the other hand, are assumed to execute boosting maneuvers over time such that they maintain their orbits until retired.

For each uncontrolled object, the altitude loss per revolution is a function of initial altitude, air density, and drag profile. The exact relationship is shown in Equation 3 [54].

$$\Delta h_{rev} = -2\pi \left(\frac{C_D A}{m}\right) \rho a^2 \tag{3}$$

where Δh_{rev} is altitude loss per revolution, C_D is drag coefficient, A is cross-sectional area, m is mass, ρ is atmospheric density, and a is the initial semi-major axis. All objects are assumed to have a typical value of $C_D = 2.2$ [49], and cross-sectional area A and mass m are already defined as described previously. Because atmospheric density ρ varies based on altitude, a density function was defined by linearly interpolating data points from an exponential atmospheric model [55]. Finally, since circular orbits are assumed throughout, semi-major axis a is simply the sum of an object's initial altitude and the Earth's radius.

Once an object's altitude loss per revolution is known, then altitude loss per time step is considered. For a given orbit, the number of revolutions in time dt [sec] is defined by Equation 4.

$$R = \frac{dt}{2\pi} \sqrt{\frac{\mu}{a^3}} \tag{4}$$

where R is the number of revolutions, μ is the Earth standard gravitational parameter, and a is again the initial semi-major axis. Multiplying the results of Equations 3 and 4 then yields the total

25

altitude loss per time step. This altitude loss is calculated for each uncontrolled object and then subtracted from the initial altitude, thus updating all orbits in the simulation. At low altitudes, orbital decay can lead to a significant "cleaning" effect as objects gradually reenter the atmosphere, but this effect is very weak at higher altitudes.

3.5   Post-Mission Disposal

Since orbital decay applies only to non-operational objects and debris, post-mission disposal is essentially the sole removal mechanism for active objects in the simulation. When first added to the population, all active objects are assigned an EOL timestamp: 10 years after launch for standard satellites and 6 years, 4 months after launch for Starlink satellites. The simulation continually compares these EOL timestamps to the current timestamp, and any active objects past their lifetime are flagged for retirement. Importantly though, a certain percentage of retiring objects will always "fail" to dispose based on the chosen success rate for PMD. A random number is generated for each retiring object, and disposal is considered successful if this number is less than the PMD rate (e.g. PMD = 50% = 0.5). For a successful disposal, the object is assumed to immediately disappear from the population. For a failed disposal, the object is stripped of its active status and added to the list of non-operational objects.

The simulation considers two distinct PMD rates, one for standard satellites and one for Starlink satellites. The success rate for standard PMD is assumed to always be 90%, a common assumption used in recent literature [33] [43]. This 90% PMD rate is admittedly optimistic given current regulatory compliance [17], but it effectively creates a best-case scenario for the LEO environment so that the effects of Starlink can be more easily studied. As discussed previously, Starlink's PMD rate is one of the independent variables being studied in this thesis, and so the test cases shown later assume values ranging from 90% to 99%.

26

3.6   Collision Analysis

Once all objects have been updated to reflect orbital decay and post-mission disposal, the simulation conducts a two-part collision analysis: first determining if on-orbit collisions occur in a given time step, and then adding any resulting debris. To begin, all objects in the simulation are sorted by altitude and then divided into 50-km orbital shells from 100 to 2000 km. The objects within a specific shell are then further subdivided into intact objects (i.e. active and non-operational objects) and debris objects, and spatial densities and average radii are found separately for each class of objects. It is also assumed that all objects can be modeled as spheres, allowing average radius to be easily computed from cross-sectional area. This assumption of spherical objects is widely used in orbital debris literature, with one study citing only a 10% difference in results compared to using more complex shapes [42]. Once the intact and debris objects in each orbital shell are characterized, a statistical approach is used to find collision probabilities.

This simulation adopts Pardini and Anselmo's method of estimating collision probabilities, which assumes three types of collisions: intact-intact, debris-intact, and debris-debris. Equations 5-7 are used to find probabilities for each collision type in each orbital shell [12].

$$CR_{i-i} = 4\pi r_i^2 \frac{\rho_i v_{rel}(\rho_i V - 1)}{2} dt \qquad (5)$$

$$CR_{d-i} = \pi (r_d + r_i)^2 \rho_d v_{rel} \rho_i V (dt) \qquad (6)$$

$$CR_{d-d} = 4\pi r_d^2 \frac{\rho_d v_{rel}(\rho_d V - 1)}{2} dt \qquad (7)$$

where *CR* is collisions per time step, r_i is the average intact radius, r_d is the average debris radius, ρ_i is the spatial density for intact objects, ρ_d is the spatial density for debris objects, *V* is the volume of the orbital shell, v_{rel} is the relative velocity, and *dt* is the time step. The relative velocity v_{rel} among cataloged objects is assumed to be 10 km/s [12], and the time step *dt* is 5 days. By applying

Equations 5-7 to each orbital shell in the simulation, one arrives at the 5-day probabilities for each collision type at evenly-spaced altitudes throughout LEO.

Once collision probabilities are known for each orbital shell, a random number generator determines if any collisions actually occur in a given time step. Three random numbers between 0 and 1 are generated for each orbital shell, and a collision is triggered if any random number is less than its corresponding collision probability (e.g. $CR_{i\text{-}i} = 0.01$). This standard trick allows the timing of collisions to follow an overall probability distribution while still varying realistically across different simulations. Next, if a collision is triggered, the two colliding objects are randomly selected from the orbital shell based on the type of collision. Importantly, the simulation assumes perfect collision avoidance for operating satellites, so a collision is ignored if either random selection is an active object. In this case, no new debris is introduced, but the event is logged as a "potential collision" in order to characterize the number of collision avoidance maneuvers that were required throughout the simulation.

On the other hand, if neither colliding object can actively avoid the collision, then a breakup occurs and introduces new debris into the environment. These events are simulated using the NASA Standard Breakup Model, a widely-used algorithm that relates the mass and velocity of colliding objects with the resulting distribution of collision fragments [56]. To apply the NASA model, it is critical to understand the distinction between "catastrophic" and "non-catastrophic" collisions. The former classification refers to events with a sufficient energy-to-mass ratio (exceeding 40 kJ/kg) to cause complete fragmentation of the colliding bodies, while collisions of the latter type generate significantly less debris [12]. Thus, before characterizing the breakup itself, the simulation first calculates the energy-to-mass ratio of the collision to determine if it is catastrophic or non-catastrophic. Here, relative velocity is again assumed to be 10 km/s.

Once a collision is characterized as catastrophic or non-catastrophic, the NASA Standard Breakup Model is applied to determine the distribution of collision fragments. Ten ranges of fragment diameters are considered: 10-20 cm, 20-30 cm, 30-40 cm, and so on, with the final range including all fragments larger than 1 meter. For each range of fragment diameters, also known as characteristic sizes, Equation 8 from the NASA Standard Breakup Model is used to estimate the number of collision fragments.

$$N(L_c) = 0.1M^{0.75}L_C^{-1.71} \tag{8}$$

where $N(L_c)$ is the number of fragments larger than the characteristic size, L_c is the characteristic size, and M follows the relationship shown in Equation 9.

$$M = \begin{cases} M_t + M_p, & \textit{if catastrophic} \\ M_p[kg] * \left(\dfrac{v_{rel}[km/s]}{1\,[km/s]}\right)^2, & \textit{if non-catastrophic} \end{cases} \tag{9}$$

where M_t is the target mass (i.e. the larger colliding mass), M_p is the projectile mass (i.e. the smaller colliding mass), and v_{rel} is the relative impact velocity [12] [56]. In summary, by applying Equations 8 and 9, the simulation is able to determine the number and approximate size of all collision-generated fragments 10 cm and larger.

Once the number of collision fragments in each size range is known, these fragments are added as debris in the overall LEO population. The altitude of all new debris is assumed to be the average altitude in the orbital shell where the collision occurred, and the assumption of spherical debris allows cross-sectional areas to be easily computed for the ten different fragment diameters noted above. Mass for each fragment diameter is calculated via a classical relationship with cross-sectional area, shown previously in Equation 1 [50]. These values for altitude, cross-sectional area, and mass are then used to add each collision fragment as a new piece of debris in the simulation's overall LEO population.

3.7 New Launches & Active Debris Removal

The final actions in each time step of the simulation are adding newly-launched objects and removing objects via active debris removal. New launches are assumed to occur together on the first day of each month, at which point the simulation identifies all standard satellites and Starlink satellites scheduled for launch in the preceding month. These newly-launched objects are then added to the LEO population as active objects. To account for industry development over the 150-year span of the simulation, the schedule also assumes a 0.5% annual growth rate for the number of standard satellites launched [48]. This assumed market growth leads to a doubling of non-megaconstellation launch activity over 150 years, with new objects being randomly selected from the entire schedule.

Active debris removal is assumed to occur annually and apply specifically to non-operational Starlink satellites that experience PMD failures. At the end of each year in the simulation, a set number of Starlink satellites are selected randomly from the non-operational population and removed. In cases where there are no remaining non-operational Starlink satellites, active debris removal is halted. For the test cases shown in the next chapter, the ADR rate varies from zero to five objects removed per year.

CHAPTER 4: RESULTS AND ANALYSIS

4.1 Evolution of LEO Debris without Megaconstellations

The first test case considered ignores megaconstellations completely, focusing solely on how the LEO debris environment would evolve over the next 150 years without disruptive technology. A total of two scenarios are considered, as shown in Figure 6 below. In the baseline scenario, launches of standard LEO satellites continue as usual with an assumed 0.5% growth rate over time. In the "no future launches" scenario, no further objects are launched into LEO once the simulation starts, though active objects continue to operate until retired. This latter scenario is not necessarily realistic, but it serves as a point of comparison to study how the LEO environment evolves with only the objects currently in orbit.
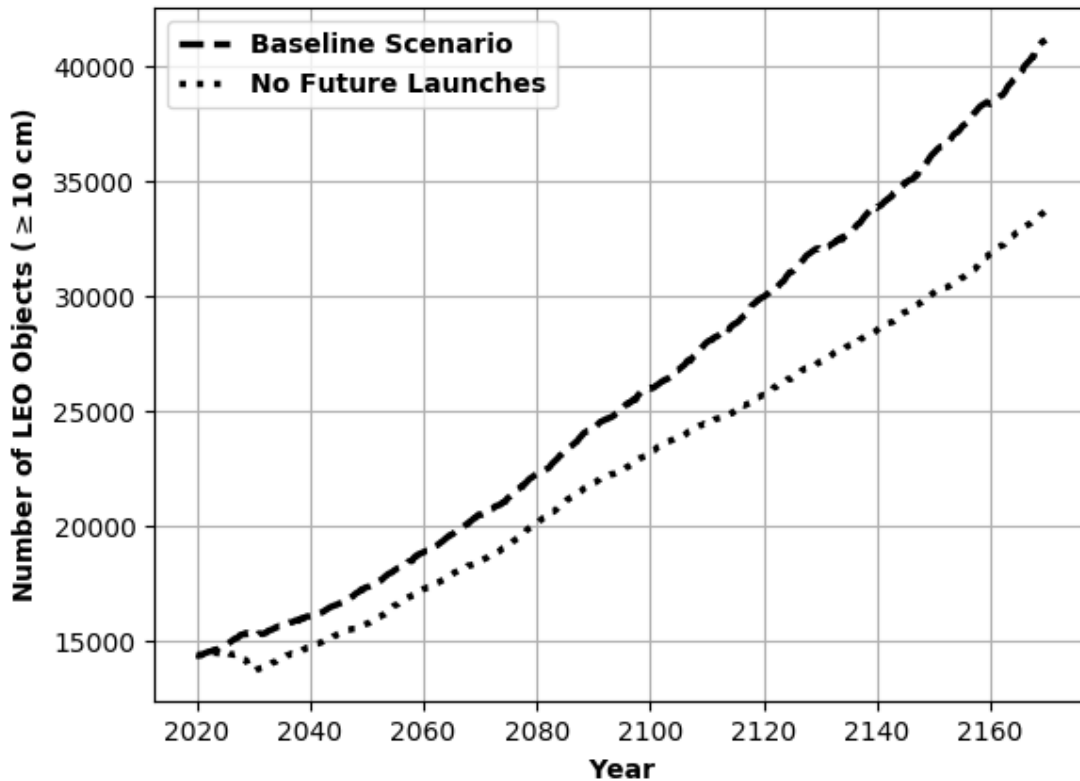

Figure 6: Evolution of LEO Objects without Megaconstellations

The goals of this first test case are twofold: to establish a baseline level of debris generation to compare against later, and to provide an opportunity to compare the new simulation against existing literature. Examining Figure 6, the results clearly demonstrate a gradual increase in the number of LEO objects for both the baseline and "no future launches" scenarios. This object growth can be attributed almost entirely to debris generation, given that 90% of any newly-launched objects are assumed to dispose successfully. In the baseline scenario, debris growth proceeds without interruption and yields a 185% increase in the number of LEO objects by 2170. The "no future launches" scenario displays a slight decrease in objects initially, as lower-altitude debris decays into the atmosphere, but growth is recovered by 2030 and ultimately leads to a 134% increase by 2170. This latter result is particularly interesting, as it suggests that debris levels will continue to increase even in a radical scenario where future launches are halted.

Since the scenarios in Figure 6 are relatively standard for an orbital debris study, this test case also serves as an opportunity to compare the new, medium-fidelity simulation against existing literature. Assuming a 90% success rate for PMD, recent simulations from the NASA Orbital Debris Program Office predict a 23 to 55% increase in the number of LEO objects over the next 150 years [33] [43], while high-fidelity simulations from Bastida Virgili et al. predict a 31% increase with an upper confidence interval of 63% [44]. Compared to these results, the new simulation in this thesis appears to predict significantly more debris generation, though the overall linear trends and orders of magnitude in Figure 6 are comparable to the high-fidelity simulations. Given the inherent uncertainties and estimations in all orbital debris studies, achieving a linear debris growth rate within the same order of magnitude as existing literature is a strong start for the new simulation. In addition, the primary goal of this thesis is to compare relative increases in debris generation, and so the simulation appears to be of sufficient accuracy.

4.2   Evolution of LEO Debris with Starlink & Varying PMD Rates

The second test case introduces the Starlink megaconstellation into the simulation, with the primary goal of studying how Starlink's PMD rate affects long-term debris growth in LEO. As discussed previously, the analysis assumes that Starlink is actively launching for 20 years and that individual Starlink satellites have a lifetime of 6 years and 4 months. Starlink's success rate for PMD is varied from 90 to 99%, and the resulting evolution of LEO debris is compared against the baseline scenario in Figure 7. The baseline scenario again assumes only the standard launch schedule, with no megaconstellations. For all scenarios shown in Figure 7, the PMD rate for standard satellites is 90%, and there is no active debris removal applied to non-operational Starlink satellites that experienced PMD failure.
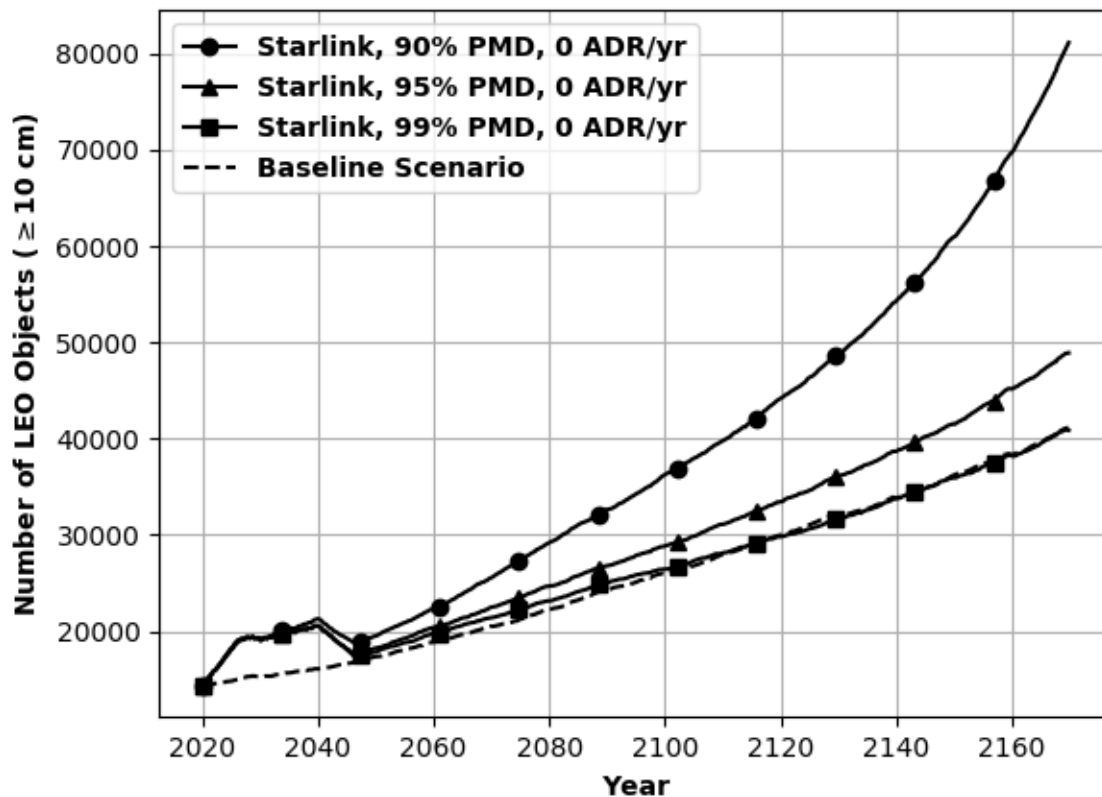

Figure 7: Evolution of LEO Objects with Starlink & Varying PMD Rates

For each of the scenarios in Figure 7, the first 20 years appear very similar. A jump in the number of LEO objects is observed from 2020 to 2026 as Starlink is first built, followed by a return to near-baseline levels once Starlink begins decommissioning in 2040. Past this point, however, both the 90% and 95% PMD cases begin to exhibit significantly enhanced debris growth compared to the baseline scenario. Table 4 displays the effects of the different PMD rates on the final LEO environment in 2170, where it can be seen that a 90% PMD rate for Starlink leads to a near doubling of LEO objects compared to the baseline scenario. This result compares very favorably with a recent NASA ODPO study, which predicted a 220% increase in LEO objects over 150 years for a megaconstellation twice as large [43]. Finally, the different trendlines in Figure 7 are also notable. While linear growth of the LEO population is maintained for PMD rates of 95% and 99%, this growth becomes exponential when PMD success is only 90%.

Table 4: Effect of Starlink PMD Rate on Final Number of LEO Objects in 2170

Starlink PMD Rate	90%	95%	99%
Change in Final Number of LEO Objects (Compared to Baseline Scenario)	+ 97.85%	+ 18.82%	- 0.81%

In comparing different PMD rates for Starlink, an additional area of interest is the effect of any newly-generated debris on operating satellites. This effect is quantified by the number of "potential collisions" with active objects throughout the simulation, which assumes that operating satellites automatically avoid collisions that would otherwise involve them. It is always desirable to minimize these potential collisions within the simulation, as in reality the assumed avoidance maneuvers consume valuable propellant and always carry a small chance of failing to prevent a collision. With this goal in mind, Figure 8 and Figure 9 display the cumulative number of potential collisions for each previously-described Starlink PMD scenario.

Figure 8 shows the number of potential collisions involving active Starlink satellites over the megaconstellation's 20-year lifespan, while Figure 9 shows the number of potential collision involving active, non-Starlink satellites over the entire 150-year simulation. Examining the effects of Starlink PMD rate in both figures, a discrepancy is apparent between short and long-term behavior. Regardless of what PMD strategy is used for Starlink, there appears to be very little change in potential collisions for both Starlink and non-Starlink satellites between 2020 and 2040. As shown in Figure 8, the number of potential collisions involving Starlink only varies by two or three when comparing the 90% and 99% PMD scenarios. In contrast, examining the post-2060 timeframe in Figure 9, the effects of Starlink's PMD strategy seem to be much more significant for non-Starlink satellites in the long term. The 90% PMD scenario, for example, adds a total of eight or nine potential collisions by 2170 compared to the baseline scenario.
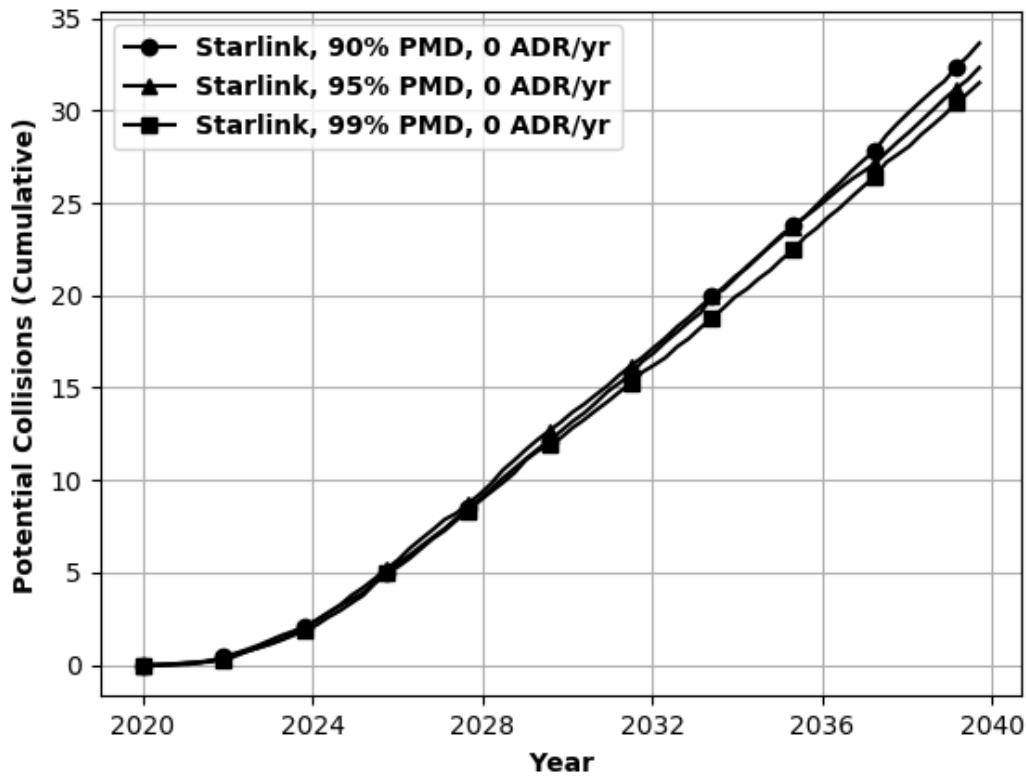

Figure 8: Potential Collisions with Starlink Satellites, for Varying Starlink PMD Rates
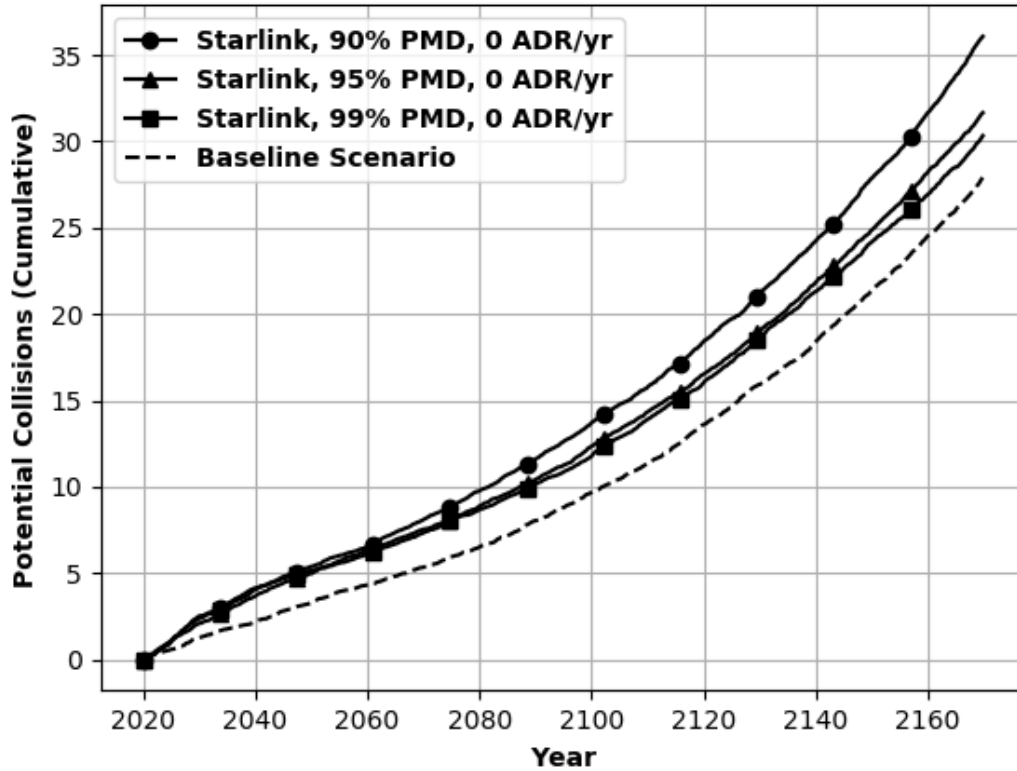
Figure 9: Potential Collisions with Non-Starlink Satellites, for Varying Starlink PMD Rates

4.3 Mitigation of Starlink-Generated Debris via Active Debris Removal

The third and final test case introduces varying levels of active debris removal to the prior test case with the Starlink megaconstellation. This active debris removal is meant to serve as a mitigation measure in instances where sub-optimal PMD rates for Starlink lead to undesirable debris growth. Since a 99% PMD rate for Starlink appears to already match the baseline scenario, as shown in Figure 7, only the 90% and 95% PMD scenarios were considered as candidates for active debris removal. The ADR rate directs the simulation to remove between 0 and 5 non-operational Starlink satellites at the end of each calendar year. Figure 10 and Figure 12 display the evolution of LEO objects assuming different levels of ADR, while Figure 11 and Figure 13 plot the corresponding numbers of LEO objects at the end of the simulation in 2170.
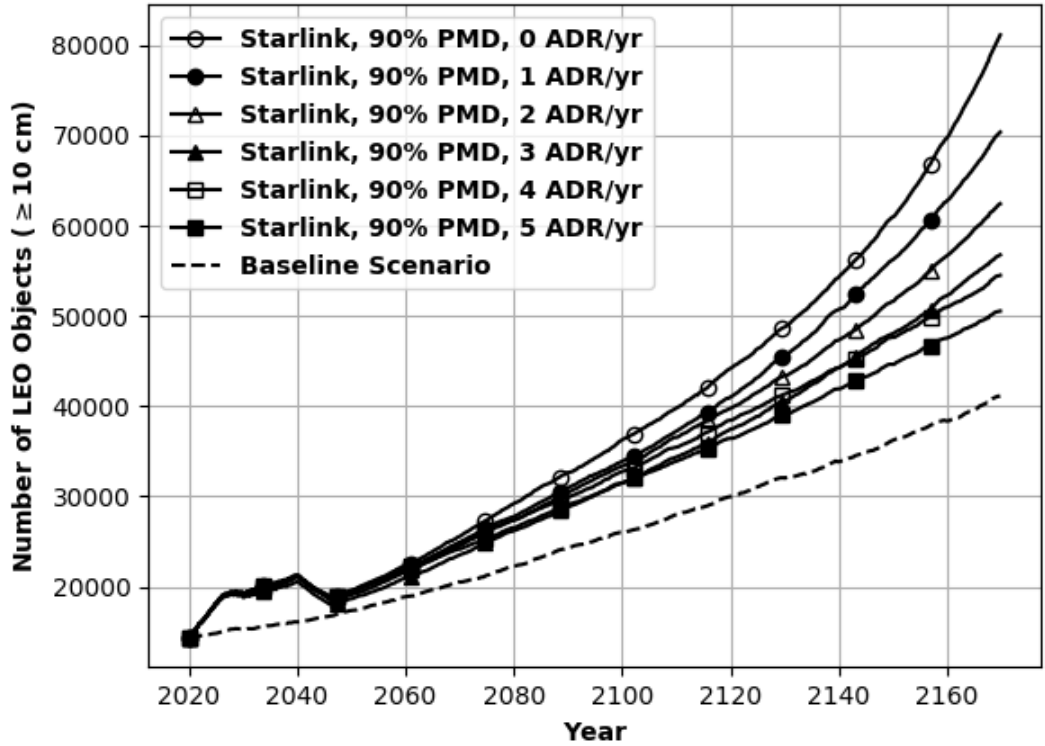
Figure 10: Evolution of LEO Objects with Varying Starlink ADR (Starlink PMD = 90%)
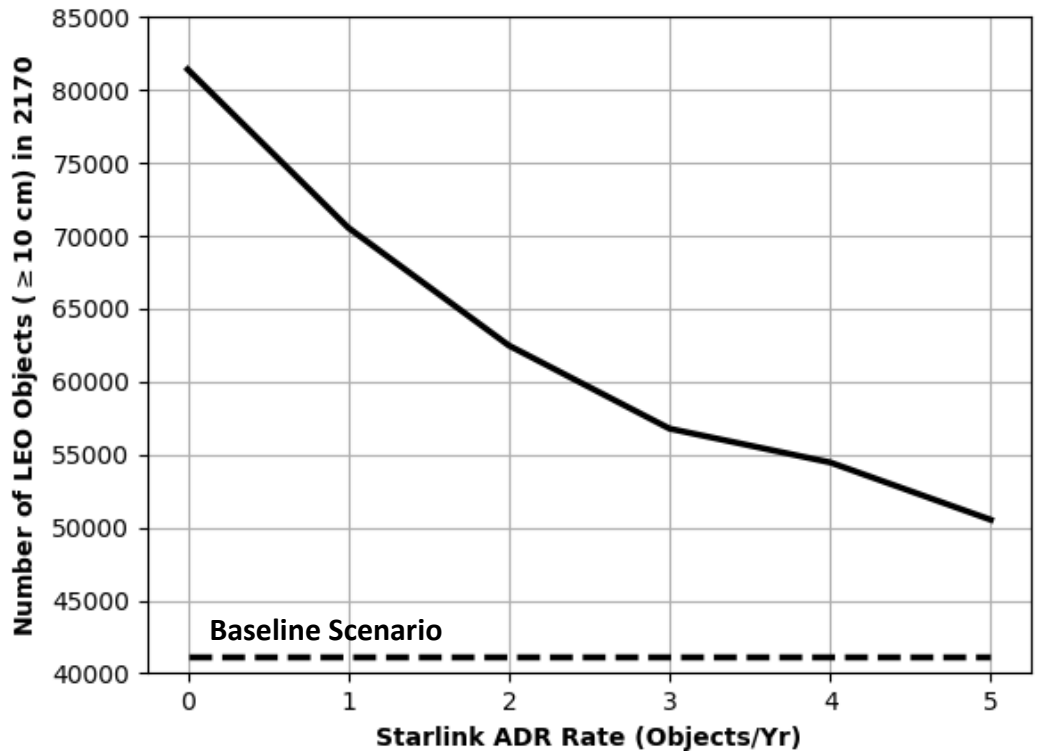

Figure 11: Effect of Starlink ADR on Final Number of LEO Objects (Starlink PMD = 90%)
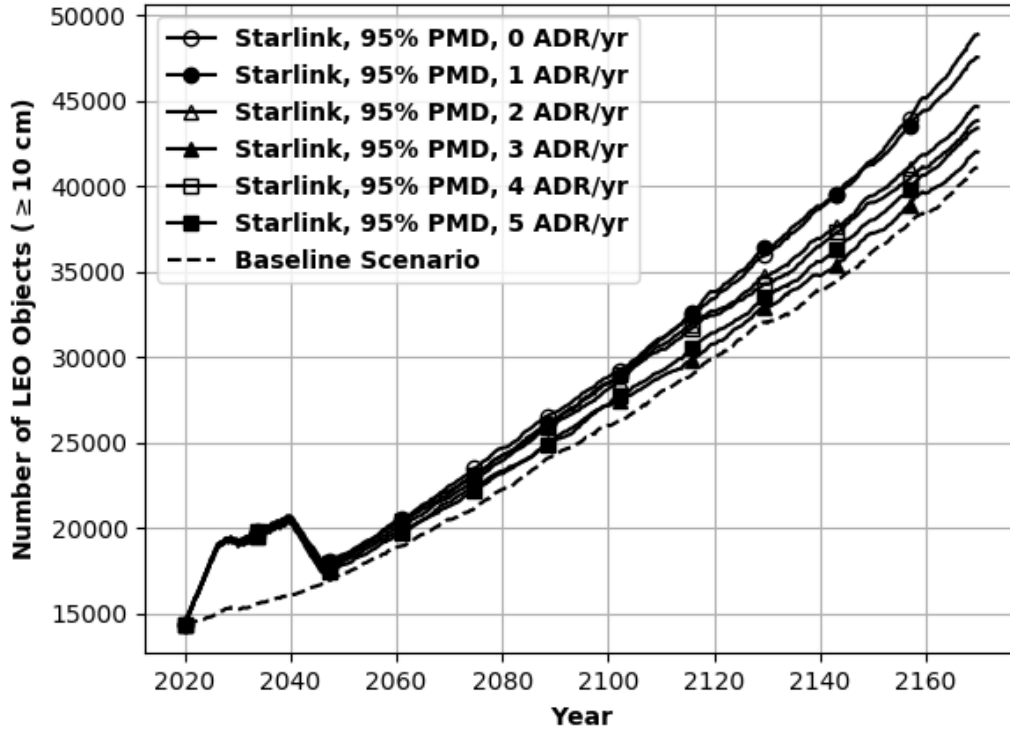
37

Figure 12: Evolution of LEO Objects with Varying Starlink ADR (Starlink PMD = 95%)
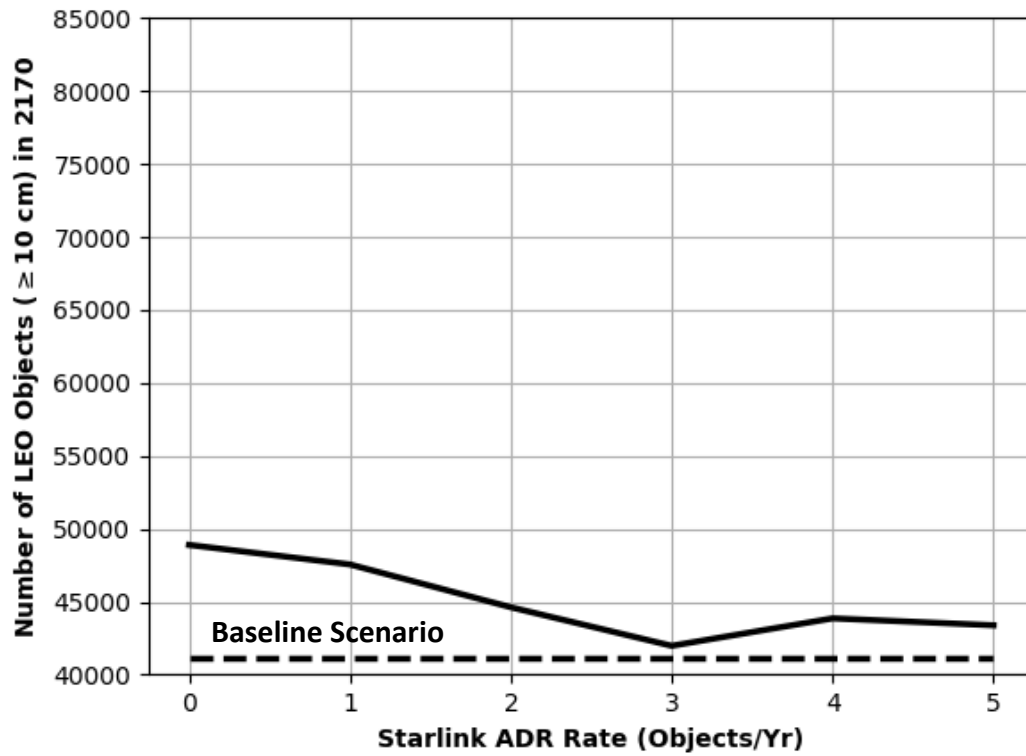

Figure 13: Effect of Starlink ADR on Final Number of LEO Objects (Starlink PMD = 95%)

38

As shown in Figure 10 and Figure 11, applying active debris removal appears to yield substantial benefits for the 90% PMD scenario. Though there appears to be diminishing returns as ADR increases in scale, the maximum considered ADR rate of 5 objects per year is still able to reduce the final number of LEO objects to levels seen for 95% PMD. This suggests that there is the potential to use active debris removal to recover from sub-optimal PMD for megaconstellations. In fact, for the 95% PMD scenario considered in Figure 12 and Figure 13, only a small amount of ADR is needed to reduce the number of LEO objects to levels seen in the baseline scenario. ADR rates beyond 3 objects per year appear to yield no substantial benefits for the 95% PMD case, and the slight increase seen in Figure 13 is likely an artifact of the inherent randomness in the Monte Carlo analysis.

CHAPTER 5: CONCLUSIONS

The results of this thesis demonstrate that satellite megaconstellations have the potential to leave a significant mark on the LEO debris environment, even centuries after they cease operations. Various test cases for the Starlink megaconstellation were analyzed in a new, medium-fidelity simulation for orbital debris evolution, and a variety of PMD and ADR rates for Starlink were considered. It was shown that if Starlink adheres only to the minimum regulatory requirement of 90% PMD for large constellations, then LEO debris levels will grow almost twice as fast as the baseline scenario with no megaconstellations. Improving Starlink's PMD rate to 95% would lead to only 19% more debris, while 99% PMD is the preferred option that prevents any significant debris contributions at all. Importantly, Starlink's choice of PMD strategy will affect its own collision risk very little over the short term, but the impact will be noticeable on multi-century timescales by the overall LEO environment. Finally, in scenarios with 90% and 95% PMD, active debris removal of non-operating Starlink satellites yields significant, if limited, benefits. The 90% PMD scenario combined with an ADR rate of 5 Starlink satellites per year, for example, is able to reduce debris levels to those seen for the 95% PMD scenario. This result suggests that active debris removal could be a viable mitigation strategy for megaconstellations with sub-optimal PMD rates.

There are several avenues to explore regarding future work for this thesis. The analysis herein could be repeated for other megaconstellations such as OneWeb and Kuiper, or the same analysis of Starlink could be conducted assuming a system lifetime beyond 20 years. In regard to active debris removal, it would be interesting to explore ADR strategies that target both standard and megaconstellation satellites – as opposed to the Starlink-only removal strategies considered in this thesis. Finally, the orbital debris simulation could be greatly improved with access to a more

detailed catalog of Earth-orbiting objects. The masses of colliding objects have a significant impact on debris evolution over time, so a better understanding of object mass in particular would be very useful. There is also the potential to enhance the speed of the simulation by incorporating parallel programming, or perhaps by saving repeated data between different Monte Carlo runs.

Speaking from a holistic perspective, the potential benefits of satellite megaconstellations cannot be ignored. Systems such as Starlink have the potential to bring about tremendous societal good in the coming decades, providing reliable and low-cost internet access to remote areas around the world. The goal of this thesis is by no means to criticize specific elements of current megaconstellations, and in fact many operators such as OneWeb and SpaceX have already taken admirable steps to reduce their debris footprints. Rather, it is hoped that such analyses offer a warning to government regulators that current guidelines for post-mission disposal and orbital lifetime may prove woefully inadequate when applied to extremely large satellite constellations.

REFERENCES

[1] Union of Concerned Scientists, "UCS Satellite Database," 16 December 2019. [Online].
     Available: https://www.ucsusa.org/resources/satellite-database. [Accessed 9 March 2020].

[2] IAF/IAA/IISL Advisory Committee on History Activities, "The History and Experience of
     the International Cospas-Sarsat Programme for Satellite-Aided Search and Rescue," 30 July
     2016. [Online]. Available: https://cospas-sarsat.int/images/content/articles/Cospas-Sarsat-
     Report_ReducedSize_Jan-2019.pdf. [Accessed 24 April 2020].

[3] National Aeronautics and Space Administration, "Orbital Debris Program Office: Frequently
     Asked Questions," NASA Johnson Space Center, [Online]. Available:
     https://orbitaldebris.jsc.nasa.gov/faq/. [Accessed 24 April 2020].

[4] Amazon, "Technical Appendix: Application of Kuiper Systems LLC for Authority to Launch
     and Operate a Non-Geostationary Satellite Orbit System in Ka-Band Frequencies," Federal
     Communications Commission, Washington, D.C., 2019.

[5] C. Henry, "OneWeb Asks FCC to Authorize 1,200 More Satellites," SpaceNews, 20 March
     2018. [Online]. Available: https://spacenews.com/oneweb-asks-fcc-to-authorize-1200-
     more-satellites/. [Accessed 27 April 2020].

[6] SpaceX, "SpaceX Non-Geostationary Satellite System, Attachment A: Technical
     Information to Supplement Schedule S," Federal Communications Commission,
     Washington, D.C., 2018.

[7] C. Henry, "Starlink Passes 400 Satellites with Seventh Dedicated Launch," SpaceNews, 22 April 2020. [Online]. Available: https://spacenews.com/starlink-passes-400-satellites-with-seventh-dedicated-launch/. [Accessed 24 April 2020].

[8] Committee on Transportation Research and Development, "Interagency Report on Orbital Debris," Library of Congress, Washington, D.C., 1995.

[9] P. Anz-Meador and D. Shoots, "Monthly Object Type Charts by Number and Mass," *Orbital Debris Quarterly News,* p. 13, May 2019.

[10] T. S. Kelso, "Satellite Catalog (SATCAT)," CelesTrak, 25 April 2020. [Online]. Available: https://celestrak.com/satcat/search.php. [Accessed 3 March 2020].

[11] M. Gruss, "U.S. Official: China Turned to Debris-Free ASAT Tests Following 2007 Outcry," SpaceNews, 11 January 2016. [Online]. Available: https://spacenews.com/u-s-official-china-turned-to-debris-free-asat-tests-following-2007-outcry/. [Accessed 26 April 2020].

[12] C. Pardini and L. Anselmo, "Review of Past On-Orbit Collisions Among Cataloged Objects and Examination of the Catastrophic Fragmentation Concept," *Acta Astronautica,* vol. 100, pp. 30-39, 2014.

[13] T. S. Kelso, "Analysis of the Iridium 33-Cosmos 2251 Collision," in *AIAA/AAS Astrodynamics Specialist Conference*, Pittsburgh, PA, 2009.

[14] European Space Agency, "Automating Collision Avoidance," 22 October 2019. [Online]. Available: https://www.esa.int/Safety_Security/Space_Debris/Automating_collision_avoidance. [Accessed 26 April 2020].

[15] SpaceNews Staff, "ISS Crew Take Shelter in Soyuz During Debris Scare," SpaceNews, 2 April 2012. [Online]. Available: https://spacenews.com/iss-crew-take-shelter-soyuz-during-debris-scare/. [Accessed 26 April 2020].

[16] U.S. Government, "Orbital Debris Mitigation Standard Practices, November 2019 Update," NASA Johnson Space Center, Houston, TX, 2019.

[17] P. B. De Selding, "OneWeb, Boeing Settle Constellation Orbit Issue; SpaceX Questions OneWeb Ownership," Space Intel Report, 25 April 2017. [Online]. Available: https://www.spaceintelreport.com/oneweb-boeing-settle-constellation-orbit-issue-spacex-questions-oneweb-ownership/. [Accessed 26 April 2020].

[18] C. Henry, "FCC Punts Controversial Space Debris Rules for Extra Study," SpaceNews, 23 April 2020. [Online]. Available: https://spacenews.com/fcc-punts-controversial-space-debris-rules-for-extra-study/. [Accessed 26 April 2020].

[19] International Telecommunications Union, "Measuring Digital Development: Facts and Figures," ITU Publications, Geneva, Switzerland, 2019.

[20] Federal Communications Commission, "Eighth Broadband Progress Report," Federal Communications Commission, Washington, D.C., 2012.

[21] C. Henry, "LEO and MEO Broadband Constellations Mega Source of Consternation," SpaceNews, 13 March 2018. [Online]. Available: https://spacenews.com/divining-what-the-stars-hold-in-store-for-broadband-megaconstellations/. [Accessed 26 April 2020].

[22] Morgan Stanley, "A New Space Economy on the Edge of Liftoff," Morgan Stanley, 12 July 2019. [Online]. Available: https://www.morganstanley.com/Themes/global-space-economy. [Accessed 26 April 2020].

[23] OneWeb, "OneWeb Files for Chapter 11 Restructuring to Execute Sale Process," 27 March 2020. [Online]. Available: https://www.oneweb.world/media-center/oneweb-files-for-chapter-11-restructuring-to-execute-sale-process. [Accessed 27 April 2020].

[24] C. Pardini and L. Anselmo, "Environmental Sustainability of Large Satellite Constellations in Low Earth Orbit," *Acta Astronautica,* vol. 170, pp. 27-36, 2020.

[25] S. Erwin, "Planet Stepping Up Marketing to Defense and Intelligence Agencies," SpaceNews, 20 November 2019. [Online]. Available: https://spacenews.com/planet-stepping-up-marketing-to-defense-and-intelligence-agencies/. [Accessed 26 April 2020].

[26] M. Safyan, "Overview of the Planet Labs Constellation of Earth Imaging Satellites," March 2015. [Online]. Available: https://www.itu.int/en/ITU-R/space/workshops/2015-prague-small-sat/Presentations/Planet-Labs-Safyan.pdf. [Accessed 26 April 2020].

[27] C. Henry, "Spire Opens Washington Office to Court Government Customers," SpaceNews, 5 November 2019. [Online]. Available: https://spacenews.com/spire-opens-washington-office-to-court-government-customers/. [Accessed 26 April 2020].

[28] H. J. Kramer, "Lemur-2 Nanosatellite Constellation of Spire Global," eoPortal Directory, [Online]. Available: https://directory.eoportal.org/web/eoportal/satellite-missions/l/lemur. [Accessed 26 April 2020].

[29] C. Henry, "Iridium Ends Legacy Satellite Service, Switches All Traffic to NEXT Fleet," SpaceNews, 6 February 2019. [Online]. Available: https://spacenews.com/iridium-ends-legacy-satellite-service-switches-all-traffic-to-next-fleet/. [Accessed 6 April 2020].

[30] Iridium, "Iridium NEXT Engineering Statement," Federal Communications Commission, Washington, D.C., 2013.

[31] C. Henry, "SpaceX Seeks FCC Permission for Operating All First-Gen Starlink in Lower Orbit," SpaceNews, 21 April 2020. [Online]. Available: https://spacenews.com/spacex-seeks-fcc-permission-for-operating-all-first-gen-starlink-in-lower-orbit/. [Accessed 27 April 2020].

[32] European Space Agency, "ESA Spacecraft Dodges Large Constellation," 9 March 2019. [Online]. Available: https://www.esa.int/Safety_Security/ESA_spacecraft_dodges_large_constellation. [Accessed 27 April 2020].

[33] J. C. Liou, N. L. Johnson and N. M. Hill, "Controlling the Growth of Future LEO Debris Populations with Active Debris Removal," *Acta Astronautica,* vol. 66, pp. 648-653, 2010.

[34] J. C. Liou, "Engineering and Technology Challenges for Active Debris Removal," in *4th European Conference for Aerospace Sciences*, Saint Petersburg, Russia, 2011.

[35] V. L. Foreman, A. Siddiqi and O. L. de Weck, "Large Satellite Constellation Orbital Debris Impacts: Case Studies of OneWeb and SpaceX Proposals," in *AIAA SPACE and Astronautics Forum and Exposition*, Orlando, FL, 2017.

[36] D. J. Kessler and B. G. Cour-Palais, "Collision Frequency of Artificial Satellites: The Creation of a Debris Belt," *Journal of Geophysical Research,* vol. 83, no. A6, pp. 2637-2646, 1978.

[37] A. Rossi, L. Anselmo, C. Pardini, P. Farinella and A. Cordelli, "Interaction of the Satellite Constellations with the Low Earth Orbit Debris Environment," in *Mission Design & Implementation of Satellite Constellations*, Toulouse, France, 1997.

[38] A. Rossi, G. B. Valsecchi and P. Farinella, "Risk of Collisions for Constellation Satellites," *Nature,* vol. 399, pp. 743-744, 1999.

[39] W. W. Mendell, D. J. Kessler and R. C. Reynolds, "Telecommunications Satellite Constellations and the LEO Debris Population," in *48th International Astronautical Congress*, Turin, Italy, 1997.

[40] L. Anselmo and C. Pardini, "Dimensional and Scale Analysis Applied to the Preliminary Assessment of the Environment Criticality of Large Constellation in LEO," *Acta Astronautica,* vol. 158, pp. 121-128, 2019.

[41] J. Radtke, C. Kebschull and E. Stoll, "Interactions of the Space Debris Environment with Mega Constellations - Using the Example of the OneWeb Constellation," *Acta Astronautica,* vol. 131, pp. 55-68, 2017.

[42] S. Le May, S. Gehly, B. A. Carter and S. Flegel, "Space Debris Collision Probability Analysis for Proposed Global Broadband Constellations," *Acta Astronautica,* vol. 151, pp. 445-455, 2018.

[43] J. C. Liou, M. Matney, A. Vavrin, A. Manis and D. Gates, "NASA ODPO's Large Constellation Study," *Orbital Debris Quarterly News,* pp. 4-7, September 2018.

[44] B. Bastida Virgili, J. C. Dolado, H. G. Lewis, J. Radtke, H. Krag, B. Revelin, C. Cazaux, C. Colombo, R. Crowther and M. Metz, "Risk to Space Sustainability from Large Constellations of Satellites," *Acta Astronautica,* vol. 126, pp. 154-162, 2016.

[45] G. A. Henning, M. E. Sorge, G. E. Peterson, A. B. Jenkin, D. Mains and J. P. McVey, "Parameterizing Large Constellation Post-Mission Disposal Success to Predict the Impact to

Future Space Environment," in *1st International Orbital Debris Conference*, Sugar Land, TX, 2019.

[46] H. G. Lewis, T. Maclay, J. P. Sheehan and M. Lindsay, "Long-Term Environmental Effects of Deploying the OneWeb Satellite Constellation," in *70th International Astronautical Congress*, Washington, D.C., 2019.

[47] S. Kawamoto, N. Nagaoka, T. Sato and T. Hanada, "Impact on Collision Probability by Post Mission Disposal and Active Debris Removal," in *1st International Orbital Debris Conference*, Sugar Land, TX, 2019.

[48] R. Klima, D. Bloembergen, R. Savani, K. Tuyls, D. Hennes and D. Izzo, "Space Debris Removal: A Game Theoretic Analysis," *Games,* vol. 7, no. 3, p. 20, 2016.

[49] R. Klima, D. Bloembergen, R. Savani, K. Tuyls, A. Wittig, A. Sapera and D. Izzo, "Space Debris Removal: Learning to Cooperate and the Price of Anarchy," *Frontiers in Robotics and AI,* vol. 5, p. 54, 2018.

[50] R. C. Reynolds, "Review of Current Activities to Model and Measure the Orbital Debris Environment in Low-Earth Orbit," *Advances in Space Research,* vol. 10, no. 3-4, pp. 359-371, 1990.

[51] G. D. Badhwar and P. D. Anz-Meador, "Relationship of Radar Cross Section to the Geometric Size of Orbital Debris," in *AIAA/NASA/DOD Orbital Debris Conference: Technical Issues & Future Directions*, Baltimore, MD, 1990.

[52] "SpaceX Non-Geostationary Satellite System, Attachment A: Technical Information to Supplement Schedule S," Federal Communications Commission, Washington, D.C., 2016.

[53] SpaceX, "Starlink Mission," April 2020. [Online]. Available: https://www.spacex.com/sites/spacex/files/seventh_starlink_mission_overview_0.pdf. [Accessed 4 May 2020].

[54] J. R. Wertz, "Orbits and Astrodynamics: Atmospheric Drag and Satellite Decay," in *Space Mission Engineering: The New SMAD*, Hawthorne, CA, Microcosm Press, 2015, pp. 214-215.

[55] R. A. Braeunig, "Atmosphere Properties," Rocket & Space Technology, [Online]. Available: http://www.braeunig.us/space/atmos.htm. [Accessed 4 May 2020].

[56] N. L. Johnson, P. H. Krisko, J. C. Liou and P. D. Anz-Meador, "NASA's New Breakup Model of EVOLVE 4.0," *Advances in Space Research,* vol. 28, no. 9, pp. 1377-1384, 2001.